A High-Order Low-Order Algorithm with Exponentially-Convergent Monte Carlo for Thermal Radiative Transfer Problems

Dissertation Proposal
Simon Bolding, Nuclear Engineering Department

July 27, 2016

1 Overview

This document describes dissertation research over a new Monte Carlo algorithm for solution of thermal radiative transfer problems. Herein, a brief description of thermal radiative transfer and the model problem are given, followed by a discussion of the standard Monte Carlo solution method and other related research. An overview of the methodology and results performed thus far are given in Sec. 3. Then, the remaining topics for completing this dissertation research are discussed in Sec. 4. Finally, Sec. 5 provides a specific outline of the remaining research to be investigated and computational results to be generated.

2 Introduction

2.1 Thermal radiative transfer background

Thermal radiative transfer (TRT) physics describe the time-dependent energy distributions of a photon radiation field and a high-temperature material. The material and radiation exchange energy through absorption and emission of photons by the material. Accurate modeling of TRT physics becomes relevant in the high-energy, high-density physics regime. Typical computational applications of TRT include simulation of inertial confinement fusion and astrophysics phenomena. The transport of photons through a material is character-

ized by particle position, direction, and frequency. The material energy distribution is described by the material internal energy (often described by material temperature) as a function of position. The high-dimensional space results in a difficult, nonlinear transport problem.

This research will focus on a simplified 1D slab-geometry and frequency-integrated (grey) TRT model. The governing equations for this simplified model are the radiation and material energy balance equations

$$\frac{1}{c}\frac{\partial I(x,\mu,t)}{\partial t} + \mu\frac{\partial I(x,\mu,t)}{\partial x} + \sigma_t I(x,\mu,t) = \frac{\sigma_s}{2}\phi(x,t) + \frac{1}{2}\sigma_a acT^4(x,t) \tag{1}$$

$$\rho c_v \frac{\partial T(x,t)}{\partial t} = \sigma_a \phi(x,t) - \sigma_a acT^4(x,t). \tag{2}$$

In the above equations the fundamental unknowns are the material temperature $T(x,t)$ and the angular intensity $I(x,\mu,t)$ of radiation, where x is the position, t is the time, μ is the x-direction cosine of the photon direction of travel, and a, c, ρ, and c_v are the radiation constant, speed of light, material mass density, and material specific heat; σ_a, σ_s, and σ_t are the absorption, scattering, and total cross sections (cm^{-1}), respectively. The scalar radiation intensity $\phi(x,t) = \int_{-1}^{1} I(x,\mu,t)\text{d}\mu$ is related to the radiation energy density E (with typical units Jks cm^{-3} sh^{-1}) by the relation $E = \phi/c$. The equations are strongly coupled through the gray Planckian emission source $\sigma_a acT^4$, which is a nonlinear function of temperature, and the radiation absorption term $\sigma_a\phi$. In general, the material properties are a function of T. The temperature dependent material properties and absorption and reemission physics lead to systems that require accurate modeling of photon transport through a mix of streaming and optically-thick, diffusive regions. Although in most physical applications material motion is present, it is not the focus of this research and will not be considered. The purpose of the proposed research is to demonstrate the ability of a new algorithm to provide highly-accurate and efficient solutions to Eq. (1) and Eq. (2).

2.2 The implicit Monte Carlo method

The Monte Carlo (MC) method [1] is a standard computational method in the field of radiation transport. The implicit Monte Carlo (IMC) method [2] is the most common approach for applying the MC method to TRT problems. The IMC method partially linearizes Eq. (1) and Eq. (2) over a discrete time step and lags material properties to produce a linear transport equation, which can be solved with MC simulation. The linear transport equation contains an approximate emission source and effective scattering cross section that represent absorption and reemission of photons over a time step. The transport equation is solved with MC simulation to advance the distribution of radiation to the end of the time step and determine the energy absorbed by the material over the time step. The energy absorption by the material is tallied over a discrete spatial mesh, computed with cell-averaged quantities. The energy absorption in each mesh cell is used to directly estimate a new end of time step material temperature based on the linearized material energy balance equation. Integration of the time-variable is treated continuously over the time step via MC sampling, but the linearized Planckian source in the transport equation is based on a time-discrete approximation.

The IMC method has some limitations. In optically thick regions, or for large time steps, the effective scattering dominates interactions. In these diffusive regions IMC becomes computationally expensive. Acceleration methods typically attempt to improve efficiency by allowing particles to take discrete steps through optically-thick regions based on a spatially-discretized diffusion approximation [3, 4]. Another issue occurs due to the approximate linearization of the system which can not be iteratively improved due to the high computational cost of the MC transport. For some problems, the linearization can yield non-physical results that violate the discrete maximum principle if the time step size is too large or the cell size is too small [5]. The violation of the maximum principle results in the material temperature being artificially higher than the boundary conditions and sources should physically allow. The violation is caused by the temperature in the emission source not being fully implicit in time due to the necessary linearization. The work in [6] uses less-expensive MC iterations to produce an implicit system which prevents this from happening, but has very

slow iterative convergence in diffusive problems. In IMC, temperature-dependent material properties, in particular cross sections, are evaluated at the previous-time step temperature. These lagged cross sections can produce inaccurate solutions but do not cause stability issues.

For TRT simulations, inaccurate spatial representation of the emission source over a cell can result in energy propagating through the domain artificially fast, yielding non-physical results referred to as "teleportation error" [7]. The IMC method uses a fixup known as source tilting to mitigate this problem. Source tilting reconstructs a more accurate linear-discontinuous representation of the emission source within a cell based on the cell-averaged material temperatures in adjacent cells. This linear reconstruction is also necessary to preserve the asymptotic equilibrium diffusion limit (EDL), at least for a more general time step size and class of problems than for a piece-wise constant representation [8]. Preserving the equilibrium diffusion limit is an important aspect of a numerical method for TRT problems. In this limit, cells are optically thick and diffusive, and the material and radiation energy fields approach equilibrium. Spatial discretizations which do not preserve the EDL can produce inaccurate solutions, even though the mesh size should accurately capture the behavior of the solution [9].

2.3 Previous work on moment-based acceleration methods

An alternative application of MC to the TRT equations is moment-based hybrid MC methods. Recent work has focused on so-called high-order low-order (HOLO) methods [10, 11, 12, 13]. These methods involve fixed-point iterations between high-order (HO) MC solution of a transport equation and a deterministic LO system. The low-order (LO) operator is based on angular moments of the transport equation, formulated over a fixed spatial mesh. Physics operators that are time consuming for MC to resolve, e.g., absorption-reemission physics, are moved to the LO system. The reduced angular dimensionality of the system and Newton methods allow for non-linearities in the LO equations to be fully resolved efficiently [10, 11]. The high-order (HO) transport problem is defined by Eq. (1), with sources estimated from the previous LO solution. The high-order (HO) transport equation is solved

via MC to produce a high-fidelity solution for the angular intensity. The MC estimate of the angular intensity is used to estimate consistency terms, present in the LO equations, that require the LO system to preserve the angular accuracy of the MC solution. These consistency terms are present in all spatial-regions of the problem, requiring statistical variance to be reduced sufficiently throughout the entire domain of the problem.

Another area of related research is the application of residual Monte Carlo. The goal of these methods is to solve an auxiliary transport equation for the error in some estimate of the intensity. The error is then added to the estimate of the solution, which can produce an overall solution for the intensity that has less statistical noise than solution of the original transport equation would produce. In [12], the MC simulation solves for the change in intensity from the previous time step. This has the potential to limit statistical noise significantly in regions where the solution is near equilibrium. The work in [12] used residual MC as a HO solver for 1D grey problems. The residual MC demonstrated impressive reduction in statistical variance. However, a piecewise constant representation was used for the space-angle representation of the intensity, which does not preserve the EDL and can be inaccurate in angularly complex regions of the problem. Similar to RMC, a difference formulation has been applied to another algorithm known as the symbolic IMC method (SIMC), for the case of 1D frequency-dependent problems [14]. SIMC forms a standard FE solution to the material energy balance equation, and uses symbolic weights in the MC transport to solve for expansion coefficents. The difference formulation modifies the transport equation to solve for unknowns representing the deviation of the intensity from equilibrium with the material energy. The difference formulation was also applied to a linear-discontinuous FE spatial representation of the emission source, demonstrating accuracy in the EDL [15]. Both [14] and [12] produced minimal statistical noise in slowly varying problems where the behavior of the system is near equilibrium.

2.4 Proposed algorithm

The research proposed herein provides a new HOLO algorithm for radiative transfer. In this work, we propose an S_2-like LO operator [16] in conjunction with an exponentially-

convergent MC (ECMC) method [17] for the HO solver. Our LO system and approach to enforcing consistency contrast greatly from the typical formulation in [12, 10, 11]. We have derived the LO operator directly from the transport equation, using a linear-discontinuous finite-element (LDFE) spatial discretization. Exponentially-convergent Monte Carlo (ECMC)[17, 13] provides an iterative algorithm that can efficiently reduce statistical noise to acceptable levels with significantly less particle histories than standard MC. In particular, ECMC is exceptionally efficient in time-dependent TRT problems because information about the intensity from the previous time step can be used as an accurate initial guess for the new end of time step intensity. However, implementation of ECMC is non-trivial, requiring a finite-element representation of the solution in all phase-space variables that are being sampled with MC. The method contains many of the desired qualities, such as preserving the equilibrium diffusion limit, preserving the maximum principle, and in particular, providing high-fidelity MC solution to the TRT equations in an efficient manner.

3 Performed Research

3.1 Overview of the HOLO Algorithm

For simplicity, our HOLO method uses a backwards Euler discretization in time, as well as constant specific heats and cell-wise constant cross sections. The time-discretized equations are

$$\mu \frac{\partial I^{n+1}}{\partial x} + \left(\sigma_t^{n+1} + \frac{1}{c\Delta t} \right) I^{n+1} = \frac{\sigma_s}{2} \phi^{n+1} + \frac{1}{2} \left(\sigma_a a c T^4 \right)^{n+1} + \frac{I^n}{c\Delta t} \tag{3}$$

$$\rho c_v \frac{T^{n+1} - T^n}{\Delta t} = \sigma_a^{n+1} \phi^{n+1} - \sigma_a a c (T^4)^{n+1}, \tag{4}$$

where Δt is the uniform time step size, the superscript n is used to indicate the n-th time step. Cross sections are evaluated at the end of time step temperature, i.e., $\sigma_a^{n+1} \equiv \sigma_a(T^{n+1})$.

In the HOLO context, the LO solver models the physical scattering and resolves the material

temperature spatial distribution $T^{n+1}(x)$, for each time step. The LO equations are formed via half-range angular and spatial moments of Eq. (3) and Eq. (4). The spatial moments are formed over a finite-element mesh and a linear-discontinuous spatial closure with upwinding is used to close the system. The angular treatment in the LO equations has the same form as those used in the hybrid-S_2 method in [16], with consistency parameters that represent angularly-weighted averages of the intensity. If the angular consistency parameters were estimated exactly, then the LO equations preserve the exact angular-averaged solution, neglecting spatial discretization errors. These consistency parameters are lagged in each LO solve, estimated from the previous HO solution for the intensity, or from a previous time step. The discrete LO equations always conserve total energy, independent of the accuracy of the consistency terms. It is noted that our LO operator is different from the nonlinear diffusion acceleration (NDA) methods used by other HOLO methods [12, 11, 10]. In NDA methods, an artificial term is added to the LO equations to enforce consistency and estimated using a previous HO solution. In our method we have simply algebraically manipulated space-angle moment equations to produce our consistency terms, which will hopefully produce more stability in optically-thick regions where NDA methods demonstrate stability issues.

The solution to the LO system is used to construct a LDFE spatial representation of the scattering and emission sources on the right hand side of Eq. (3). This HO transport problem represents a characteristic method that uses MC to invert the continuous streaming plus removal operator with an LDFE representation of sources. We will solve this transport problem using ECMC [17]. The output from ECMC is $\tilde{I}^{n+1}(x,\mu)$, a space-angle LDFE projection of the exact solution for $I^{n+1}(x,\mu)$. Once computed, $\tilde{I}^{n+1}(x,\mu)$ is used to directly evaluate the necessary consistency parameters for the next LO solve. The HO solution is not used to directly estimate a new material temperature, which eliminates typical operator splitting stability issues that require linearization of the emission source in Eq. (1).

The process of performing subsequential HO and LO solves, within a single time step, can be repeated to obtain an increasingly accurate solution for $\phi^{n+1}(x)$ and $T^{n+1}(x)$. Thus, the HOLO algorithm, for the n-th time step, is

1. Perform a LO solve to produce an initial guess for $T^{n+1}(x)$ and $\phi^{n+1}(x)$, based on consistency terms estimated with $\tilde{I}^n$.
2. Solve the HO system with ECMC for $\tilde{I}^{n+1}(x,\mu)$, based on the current LO estimate of emission and scattering sources.
3. Compute new LO consistency parameters with $\tilde{I}^{n+1}$.
4. Solve the LO system with HO consistency parameters to produce a new estimate of ϕ^{n+1} and T^{n+1}.
5. Optionally repeat 2 – 4 until desired convergence is achieved.
6. Store $\tilde{I}^n \leftarrow \tilde{I}^{n+1}$, and move to the next time step.

The consistency terms force the HO and LO solutions for $\phi^{n+1}(x)$ to be consistent to the order of the current HOLO iteration error, as long as the LDFE spatial representation can accurately represent $\phi(x)$ and $T(x)$.

3.2 The Low-Order Equations

This section contain explicit details of the LO operator. To form the LO system of equations, spatial moments are taken over each spatial cell i: $x \in [x_{i-1/2}, x_{i+1/2}]$, weighted with the standard linear finite element (FE) interpolatory basis functions. For example, the L moment operator is defined by

$$\langle\cdot\rangle_{L,i} = \frac{2}{h_i}\int_{x_{i-1/2}}^{x_{i+1/2}} b_{L,i}(x)(\cdot)\mathrm{d}x, \tag{5}$$

where $h_i = x_{i+1/2} - x_{i-1/2}$ is the width of the spatial element and $b_{L,i}(x) = (x_{i+1/2} - x)/h_i$ is the FE basis function, for cell i, corresponding to position $x_{i-1/2}$. The right moment $\langle\cdot\rangle_{R,i}$ is defined with weight function $b_{R,i}(x) = (x - x_{i-1/2})/h_i$. To reduce the angular dimensionality, positive and negative half-range integrals of the angular intensity are taken. The half-range averages of I are defined as $\phi^+(x) = \int_0^1 I(x,\mu)\mathrm{d}\mu$ and $\phi^-(x) = \int_{-1}^0 I(x,\mu)\mathrm{d}\mu$, respectively. Thus, in terms of half-range quantities, $\phi(x) = \phi^-(x) + \phi^+(x)$.

Pairwise application of the L and R basis moments with the $+$ and $-$ half-range integrals to Eq. (3) ultimately yields four moment equations per cell. As in [16], algebraic manipulation is performed to form intensity-weighted averages of μ, which we denote consistency terms. As an example, the equation resulting from application of the L moment and positive half-range integral is

$$-2\mu_{i-1/2}^{n+1,+}\phi_{i-1/2}^{n+1,+}+\{\mu\}_{L,i}^{n+1,+}\langle\phi\rangle_{L,i}^{n+1,+}+\{\mu\}_{R,i}^{n+1,+}\langle\phi\rangle_{R,i}^{n+1,+}+\left(\sigma_{t,i}^{n+1}+\frac{1}{c\Delta t}\right)h_i\langle\phi\rangle_{L,i}^{n+1,+}$$
$$-\frac{\sigma_{s,i}h_i}{2}\left(\langle\phi\rangle_{L,i}^{n+1,+}+\langle\phi\rangle_{L,i}^{n+1,-}\right)=\frac{h_i}{2}\langle\sigma_a^{n+1}acT^{n+1,4}\rangle_{L,i}+\frac{h_i}{c\Delta t}\langle\phi\rangle_{L,i}^{n,+}, \quad (6)$$

where the $\phi_{i-1/2}^{+}$ and $\mu_{i-1/2}^{+}$ terms represent face-averaged quantities at $x_{i-1/2}$. The negative direction and R moment equations are derived analogously. The element-averaged angular consistency terms are defined in terms of half-range integrals, e.g.,

$$\{\mu\}_{L,i}^{n+1,+}\equiv\frac{\langle\mu I^{n+1}\rangle_{L,i}^{+}}{\langle I^{n+1}\rangle_{L,i}^{+}}=\frac{\frac{2}{h_i}\int_0^1\int_{x_{i-1/2}}^{x_{i+1/2}}\mu\, b_{L,i}(x)I^{n+1}(x,\mu)\mathrm{d}x\mathrm{d}\mu}{\frac{2}{h_i}\int_0^1\int_{x_{i-1/2}}^{x_{i+1/2}}b_{L,i}(x)I^{n+1}(x,\mu)\mathrm{d}x\mathrm{d}\mu}. \quad (7)$$

The $\mu_{i-1/2}^{n+1,+}$ term is defined analogously and represents an angular average on the face at $x_{i-1/2}$.

To derive the LO material energy equations, $T(x)$ is represented spatially in the LDFE trial space, i.e., $T(x)\simeq T_{L,i}b_{L,i}(x)+T_{R,i}b_{R,i}(x), \quad x\in(x_{i-1/2},x_{i+1/2})$. Similarly, the emission term is represented in the material and radiation equations with the LDFE interpolant $T^4(x)\simeq T_{L,i}^4b_{L,i}(x)+T_{R,i}^4b_{R,i}(x)$. The L and R spatial moments are taken of the material energy equation, using these definitions for $T(x)$ and $\sigma_a acT^4(x)$ to simplify moments. For example, the final LO material energy equation resulting from application of the L moment is

$$\frac{\rho_i c_{v,i}}{\Delta t}\left[\left(\frac{2}{3}T_{L,i}+\frac{1}{3}T_{R,i}\right)^{n+1}-\left(\frac{2}{3}T_{L,i}+\frac{1}{3}T_{R,i}\right)^{n}\right]+\sigma_{a,i}^{n+1}\left(\langle\phi\rangle_{L,i}^{+}+\langle\phi\rangle_{L,i}^{-}\right)^{n+1}$$
$$=\sigma_{a,i}^{n+1}ac\left(\frac{2}{3}T_{L,i}^4+\frac{1}{3}T_{R,i}^4\right)^{n+1}. \quad (8)$$

Cross sections have been assumed constant over each element, evaluated at the average temperature within the element, i.e., $\sigma_{a,i}^{n+1} = \sigma_{a,i}([T_{L,i}^{n+1} + T_{R,i}^{n+1}]/2)$.

3.3 Closing the LO equations

The six degrees of freedom (DOF) over each cell i are the four moments $\langle\phi\rangle_{L,i}^{+}$, $\langle\phi\rangle_{R,i}^{+}$, $\langle\phi\rangle_{L,i}^{-}$, and $\langle\phi\rangle_{R,i}^{-}$ and the two spatial edge values $T_{L,i}$ and $T_{R,i}$. The relation between the volume and face averaged quantities and the angular consistency parameters (e.g., Eq. (7)) are not known a priori. Currently, to close the LO system spatially, the standard LDFE approximation with upwinding is used. For example, for positive flow (e.g., Eq. (6)) the face terms $\mu_{i-1/2}$ and $\phi_{i-1/2}$ are upwinded from the previous cell $i-1$ or from a boundary condition; the terms at $x_{i+1/2}$ are linearly extrapolated, computed using the L and R basis moments, e.g., $\phi_{i+1/2}^{+} = 2\langle\phi\rangle_{R}^{+} - \langle\phi\rangle_{L}^{+}$. We will investigate using the HO solution to estimate the spatial closure, as discussed in Sec. 4 A lagged estimate of I^{n+1} from the latest HO solve is used to estimate the angular consistency parameters.

3.4 Solution of the LO equations

Newton's method is used to solve the global system of coupled LO equations, based on a typical linearization of the Planckian source with cross sections evaluated at lagged temperatures. This procedure is described in [9]. Once the system is linearized, a discrete matrix equation is formed. Scattering (including the effective scattering resulting from the linearization of the Planckian source) can be included in the system matrix, producing an asymmetric, banded-matrix. The matrix has a band width of seven and is inverted directly. Newton iterations are repeated until $\phi^{n+1}(x)$ and $T^{n+1}(x)$ are converged to a desired relative tolerance.

3.5 The ECMC High Order Solver

The transport equation to be solved by the HO solver is

$$\mu\frac{\partial I^{n+1}}{\partial x}+\left(\sigma_t+\frac{1}{c\Delta t}\right)I^{n+1}=\frac{\sigma_s}{2}\phi_{LO}^{n+1}+\frac{1}{2}\left(\sigma_a acT_{LO}^4\right)^{n+1}+\frac{\tilde{I}^n}{c\Delta t}, \tag{9}$$

where the emission and scattering sources are known from the previous LO solution and $\tilde{I}^n$ is the LDFE projection of $I(x,\mu)$ from the previous time step. This defines a fixed-source, pure absorber transport problem that must be solved for each HO solve. In operator notation, Eq. (9) can be written as

$$\mathbf{L}I^{n+1}=q \tag{10}$$

where I^{n+1} is the exact transport solution for the end-of-time-step intensity. The linear operator $\mathbf{L}$ is the streaming plus removal operator defined by the left hand side of Eq. (3). The m-th approximate LDFE solution to Eq. (10) (m is the index of inner HO batches) is represented as $\tilde{I}^{n+1,(m)}$. The m-th residual is defined as $r^{(m)}=q-\mathbf{L}\tilde{I}^{n+1,(m)}$. Addition of $\mathbf{L}I^{n+1}-q=0$ to the residual equation and manipulation of the result yields the error equation

$$\mathbf{L}(I^{n+1}-\tilde{I}^{n+1,(m)})=\mathbf{L}\epsilon^{(m)}=r^{(m)} \tag{11}$$

where I^{n+1} is the exact solution and $\epsilon^{(m)}$ is the error in $\tilde{I}^{n+1,(m)}$. We have suppressed the HOLO iteration indices because the LO estimated q^k and $\mathbf{L}^k$ remain constant over the entire HO solve. The $\mathbf{L}$ operator in the above equation is inverted yielding the Monte Carlo LDFE projection of the error in $\tilde{I}^{n+1,(m)}$, i.e.,

$$\tilde{\epsilon}^{(m)}=\mathbf{L}^{-1}r^{(m)} \tag{12}$$

where $\mathbf{L}^{-1}$ is the inversion of the streaming and removal operator via MC simulation. The fundamental transport of particles is the same as standard MC particle transport codes, but the LDFE source will now contain positive and negative weight particles. The space-angle moments of the computed error $\tilde{\epsilon}^{(m)}$ can be added to the moments of $\tilde{I}^{n+1,(m)}$ to produce a more accurate solution.

Here, we emphasize the solution $\tilde{I}^{n+1,(m)}$ represents the projection of the exact Monte Carlo solution onto the LDFE trial space. This is in general far more accurate than a standard finite element solution, particularly in the angular variable. For example, in typical IMC calculations the average energy deposition within a cell is computed using a standard path-length volumetric flux tally; the zeroth moment of the LDFE projection of $\tilde{\epsilon}$ is computed using an equivalent tally. The primary truncation error is in the LD spatial representation of the source term q. Volumetric flux tallies over each space-angle element are required to represent $\tilde{\epsilon}^{(m)}$.

The ECMC algorithm is

1. Initialize guess for $\tilde{I}^{n+1,(0)}$ to $\tilde{I}^{n}$ or the projection of $\tilde{I}^{n+1}$ from the latest HO solve
2. Compute $r^{(m)}$.
3. Perform a MC simulation to obtain $\tilde{\epsilon}^{(m)} = \mathbf{L}^{-1} r^{(m)}$
4. Compute a new estimate of the intensity $\tilde{I}^{n+1,(m+1)} = \tilde{I}^{n+1,(m)} + \tilde{\epsilon}^{(m)}$
5. Repeat steps 2 – 4 until desired convergence criteria is achieved.

The initial guess for the angular intensity $I^{n+1,(0)}$ is computed based on the previous solution for $\tilde{I}^{n}$. This is a critical step in the algorithm; it significantly reduces the required number of particles per time step because the intensity does not change drastically between time steps in optically thick regions. Exponential convergence is obtained because with each batch a better estimate of the solution is being used to compute the new residual, decreasing the magnitude of the MC residual source each iteration m, relative to the solution I^{n+1}. Each MC estimate of the moments of ϵ still has a statistical uncertainty that is governed by the standard $1/\sqrt{N}$ convergence rate [1], for a particular source $r^{(m)}$, where N is the number of histories performed. If the statistical estimate of the projection $\tilde{\epsilon}$ is not sufficiently accurate, then the iterations would diverge.

Because the exact angular intensity does not in general lie within the LDFE trial space, the iterative estimate of the error will eventually stagnate once the error cannot be sufficiently represented by a given FE mesh. An adaptive $h-$refinement algorithm has been

implemented that can be used to allow the system to continue converging towards the exact solution [17, 13]. In general, for TRT problems, optically thick and slowly varying regions of the problem do not require as refined of a mesh as neutronics calculation to accurately capture the solution because there is less variation in the angular dependence of the solution. It is noted the adaptive refinement is only applied to the HO mesh; the LO spatial mesh is fixed.

We have applied some basic variance reduction techniques. Because we are solving a pure absorber problem with Monte Carlo, we will allow particles to stream without absorption to reduce statistical variance in the tallies. The weight of particles is reduced deterministically along the path as they stream, with no need to sample a path length. Another implemented variance reduction is biased source sampling locations. The goal is to effectively distribute particle histories to regions of importance, but to sample a minimum number of histories in less probable regions to prevent large statistical noise. However, there is no need to sample histories where the solution is in equilibrium. The importance sampling is performed using a modified systematic sampling method [1].

3.6 Computational Results

The research described thus far has been implemented in a stand alone research code. To demonstrate the efficacy of our algorithm, we provide results of our HOLO algorithm for two Marshak wave test problems. Marshak wave problems provide a standard test for computational methods in radiative transfer. For the first problem, the radiation and material energies are initially in equilibrium at a cold temperature. A large, isotropic incident intensity is applied at $x = 0$. The absorption cross section varies as $\sigma(T) = 0.001\ \rho\ T^{-3}$ (cm^{-1}). The simulation is advanced until $t = 5$ sh (1 sh $\equiv 10^{-8}$ s) with a fixed time step size of 0.001 sh. We have performed no mesh refinement, only performed one HOLO iteration per time step, and used a fixed 3 HO batches with equal number of histories per batch. Radiation energy distributions are plotted as an equivalent temperature given by $T_r = (\phi/(ac))^{0.25}$. Cell-averaged quantities are plotted.

Fig. 1a compares the cell-averaged radiation temperatures for IMC with source tilting and the HOLO method with ECMC, for various number of spatial mesh cells N_c; we have used HOLO-ECMC to denote our algorithm because later results will use different HO solvers. The IMC and HOLO solutions agree as the mesh is converged. Fig. 1b compares solutions for the case of 200 cells. The HOLO method demonstrates significantly less statistical noise, even though it used fewer histories per time step. To prevent negativities in the LO equations, a modified spatial closure was used that is equivalent to the standard FE lumping procedure. This lumping-equivalent closure and S_2 equivalent consistency terms are applied in cells where negative values occur to ensure positivity. An alternative approach to resolving negativities is proposed in Sec. 4.1.

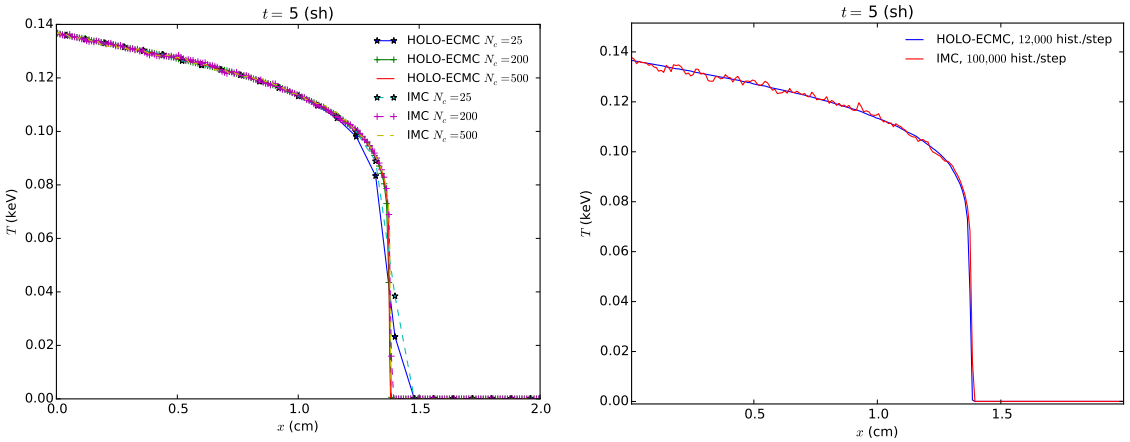

(a) Spatial convergence of IMC and HOLO. **(b)** Comparison of solutions for 200 spatial cells.

Figure 1: Comparison of radiation temperatures for Marshak wave problem at t = 5 sh.

The second problem has similar behavior to the first problem, however the geometry consists of an optically thin (left) and an optically thick (right) material region, with temperature-independent cross sections. Fig. 2a compares the HOLO and IMC radiation temperatures at the end of the simulation. The IMC and HOLO results show good agreement over the finer mesh. On the coarse mesh ($N_c = 20$), the LDFE representation of T^4 in the HOLO method predicts the location of the wave front more accurately than the source tilting of the IMC method. Fig. 2b demonstrates the benefit of ECMC as a HO solver compared to standard MC. The HOLO algorithm with the ECMC HO solver (HOLO-ECMC) results are for

running 3 batches of 10,000 histories, per time step. The solution for the HOLO method with a standard MC solver as the HO solver (HOLO-SMC) with standard source sampling uses 10^5 histories per time step. The HOLO-SMC solution demonstrates significant statistical noise. This noise is introduced into the LO solver by poor statistics in the MC computed consistency terms. Also plotted is an S_2 solution obtained with consistency terms that are equivalent to S_2 and no HO correction. The S_2 solution results in an artificially fast wave front, as expected, demonstrating the necessity of HO correction in this problem.

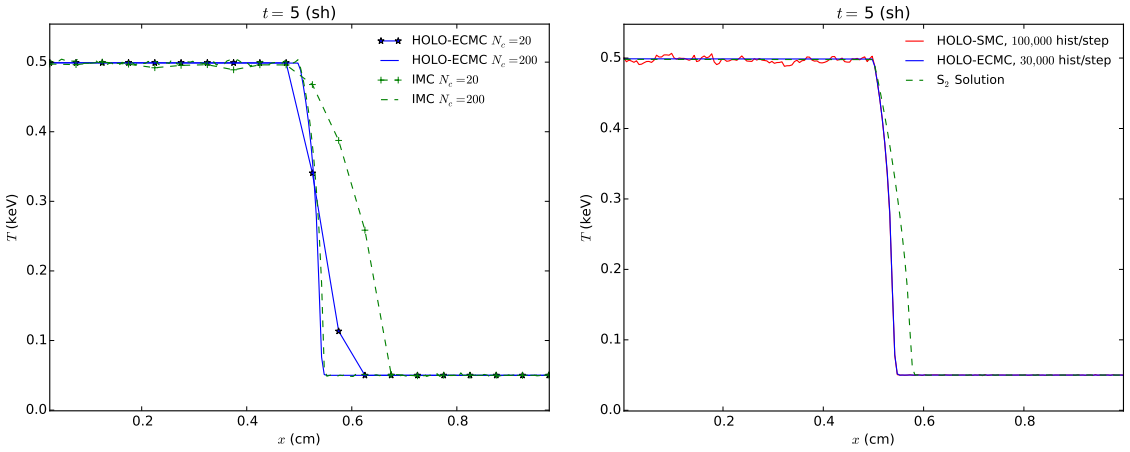

(a) Comparison of IMC and HOLO-ECMC. **(b)** Comparison of SMC and ECMC HO solvers.

Figure 2: Comparison of radiation temperatures for two material problem.

4 Discussion of Remaining Research

4.1 Resolving Issues in Optically Thick Cells

The linear-discontinuous (LD) closure with upwinding is not strictly positive. In particular, for optically thick cells with a steep intensity gradient, the intensity becomes negative. In typical TRT problems (e.g., the Marshak wave problems above), this negativity occurs at the wave-front of the radiation intensity in optically thick materials. These negativities are not physical and can propagate to adjacent cells. In thick regions of TRT problems, reasonably fine spatial cells can still be on the order of millions of mean free paths; negativities with

an LD representation are unavoidable in practice for such cells, and mesh refinement is of minimal use. We will explore several methods for resolving negativities. Ideally the solutions in such cells should be as consistent as possible for the HO and LO equations. However, the differences between the solution methods of the two equations, as well as the fact that some terms are lagged, have lead to the development of independent approaches for the LO and HO systems thus far.

Typically, for a standard LDFE method, the equations are lumped to produce a strictly positive solution (for 1D) [9]. However, standard FE lumping procedures would introduce difficulties in computing the consistency terms from the HO solution. The results in Sec. 3.6 used a lumping-equivalent closure for the LO equations and S_2 equivalent angular terms.. This approach will not produce accurate results for general problems in higher spatial dimensions. Also, a lumping equivalent closure in x does not guarantee positivity for the space-angle LDFE representation of the HO intensity. Alternatively, the equations within a cell can be modified to ensure the outflow is not below the floor value (the initial temperature of the problem), and energy balance is conserved. The LD shape is reconstructed by extrapolating from the outflow back through the average. This closure has been implemented and is more promising for extendability into higher dimensions.

For the HO solver, after an ECMC batch, we detect cells that produced a negative intensity. In these cells, we scale the linear representation of the intensity (in x and μ) to be greater than the floor value. This scaling process of the two moments is underdefined, so there is not a unique way to enforce positivity. The scaling procedure is not an emphasis of the research, so we apply the simple approach of scaling the slopes such that the ratio of the slope in x and μ is unchanged. The scaled intensity will not satisfy the original residual equation accurately because we have modified the first moments. Thus, the ECMC error estimates will rapidly stagnate, and produce relatively inaccurate solutions. This scaling can also lead to negativities in down-stream cells that is unphysical in later batches. To mitigate stagnation and improve accuracy, we will add an artifical source $\tilde{\delta}^{m+1}(x, \mu)$ to the

HO equation. This source is estimated iteratively as

$$\tilde{\delta}(x,\mu)^{(m+1)} = \mathbf{L}(\tilde{I}^{n+1,(m)} - \tilde{I}^{n+1,(m)}_{\text{pos}}),$$

where $\tilde{I}^{n+1}_{pos}$ is the modified positive solution. The goal of this modified transport problem is to maintain the zeroth moment of the solution, while modifying the slope of the solution such that the ECMC solution is converging towards a positive solution, at the rate the mesh resolution allows. If necessary, we can estimate a new source again in the next batch. The source $\tilde{\delta}$ lies in the same functional space as the residual, and thus can use the existing code for computing the residual and will be straight forward to extend to higher dimensions.

We have implemented this artificial source and found it to reduce the magnitude of the MC estimated error, producing a positive solution. We still need to investigate the accuracy and robustness of the added source method, and whether it should be recomputed every batch, once it has been triggered, or only when the solution becomes negative again. We will also investigate this source in conjuction with a modified trial space obtained by extrapolating the MC solution on an outflow face through the interior of the solution. The next section explains how the solution on faces is computed.

4.2 Estimating the Spatial Closure from the HO Solution

We will explore the possibility of a linear, doubly-discontinuous trial space in in the HO and LO equations. This trial space allows the outflow from a cell to be discontinuous in space, introducing extra unknowns. The linear shape on the interior of the cell is still used to represent the temperature unknowns, scattering source, and emission source. The choice of this trial space should allow for higher consistency between the HO and LO equations by using MC to compute outflows from space-angle cells, rather than an LD extrapolation of the solution. For the HO solution, a discontinuous outflow for a space-angle cell should produce greater angular accuracy on faces. In optically thick cells, this will mitigate observed issues with the spatial slope being artificially high to account for the discrepancy in angular shape

between the internal and face solutions. The outflow will be estimated using a face-based tally of the MC solution. The error equation can be modified to estimate the outflow for a given batch. For the LO equations, a parametric relation between the outflow and internal moments, as estimated by the latest HO solution, will be used to eliminate the extra unknowns. This will produce a consistent spatial closure between the HO and LO solutions upon convergence. The closure relation will be averaged over each half-range, similar to the angular consistency parameters. Poor statistics for the face tallies may result in this trial space producing less accurate results compared to the standard LDFE solution, at least for sufficiently fine meshes where LD can accurately represent the solution. Although the closure will be applied everywhere, we expect the greatest improvement in accuracy for cells where the LDFE trial space produces a negative solution.

4.3 Inclusion of the Time Variable in ECMC Trial Space

We hope to remove some of the error of the time trial space by including the time variable in the trial space for ECMC. Thus, our L operator is now modified to include the time derivative, i.e.,

$$LI = \frac{1}{c}\frac{\partial I}{\partial t} + \sigma_t I + \mu\frac{\partial I}{\partial x} \tag{13}$$

4.4 Diffusion Synthetic Acceleration of the LO Equations

As described in Sec. 3.4, the fully-discretized LO equations can include the scattering term in the system matrix. This allows for the system to be directly inverted. However, the S_2 like system cannot be efficiently inverted directly in higher spatial dimensions. To demonstrate a possible path forward in higher dimensions, we will investigate the use of a standard source iteration scheme to solve the LO equations. As material properties become more diffusive (e.g., c_v is small and σ_a is large), the effective scattering source becomes large. This results in a spectral radius of the source iterations that approaches unity [9]. These regimes are typical in TRT simulations, so an acceleration method is critical. We will accelerate the source iterations with a nearly-consistent diffusion synthetic acceleration

(DSA) method [18, 19].

We can perform standard source iterations by lagging the scattering source in the LO equations, which uncouples unknowns between the two half-ranges. This produces a lower-triangular system where the spatial unknowns can be determined sequentially along the two directions of flow via a standard sweeping procedure [20, 9]. The newly computed half-range intensities can be used to compute the scattering source for the next iteration. This process is repeated until convergence. A form of DSA referred to as the WLA method is used to accelerate the source iterations [18]. Between each source iteration, a residual equation is formed that provides the error in the current scattering iteration. The DSA method uses an approximate, lower-order operator to estimate the error in the zeroth angular moment of the intensity. The DSA equations can be more efficiently solved than the S_2-like sweeps that are being accelerated, but will accurately resolve the slowly converging diffusive error modes. It is important for the spatial discretization of the DSA equations to be closely related to the discretization of the LO equations for the acceleration to be effective. The WLA method first solves a spatially-continuous discretization of the diffusion equation for the iterative error on faces. The error on the faces is then mapped onto the volumetric moment unknowns via a LD discretization of diffusion equation [18]. The LD mapping resolves issues that would occur in optically-thick cells, while the continuous diffusion equation is accurate in the EDL where acceleration is important.

We have implemented the DSA algorithm and initial results indicate that the acceleration is effective. However, we have only considered the case when the LO equations and DSA equations are lumped. We will investigate the effect of acceleration when alternative negativity fix-ups are implemented that result in DSA and LO equations that are not spatially consistent. We will recast the DSA method as a preconditioner to an iterative Krylov solution [21] of the LO equations if acceleration degrades. Generally, Krylov methods mitigate acceleration losses due to inconsistencies in the acceleration method. In higher dimensions, the use of a Krylov method is necessary for effective acceleration for nearly-consistent acceleration methods such as WLA in problems with mixed optical thicknesses [21], e.g., typical radiative transfer problems. We would apply the preconditioned-Krylov approach to allow

for the use of lumped DSA equations as a preconditioner, with the LO equations using one of the other fixup approaches detailed in the previous section. It is noted we are not interested in measuring the reduction of computational time because in 1D the LO equations can be directly solved efficiently. We are just interested in ensuring that DSA or a preconditioned-Krylov methods can reduce the number of scattering iterations sufficiently, including cases where inconsistencies in the LO equations are present.

5 Summary and Outline of Remaining Research

A new HOLO algorithm has been implemented, and results have demonstrated the ability to reproduce IMC solutions accurately for two difficult Marshak wave test problems. The ECMC approach, with initial guesses based on the previous radiation intensity, results in efficient reduction of statistical error and allows for particles to be distributed to largely varying regions of the problem. The LO solver resolves the non-linearities in the equations resulting in a fully implicit time discretization. Overall, the LO solver can accurately and efficiently resolve the solution in diffusive regions, while the HO transport solver provides the accuracy of a full transport treatment where necessary.

We have proposed solutions to resolve issues in optically-thick cells and a source iteration method for demonstrating the efficacy of our method. The ability to overcome rapid stagnation in the ECMC algorithm when the solution cannot be accurately represented by the trial space, e.g., negativities in optically thick cells, will be key for generalization of this method to higher dimensions. The goal of our proposed fixup is to mitigate the rapid stagnation of ECMC iterations that would occur by forcing a positive solution each batch. Ideally, the added source will reduce the stagnation to order of the global stagnation that occurs in other regions of the problem due to mesh resolution and a finite number of histories per batch. The LO and HO solutions will independently resolve issues with negativities, with the goal of producing as consistent and accurate of solutions as possible. We also need to numerically demonstrate the ability of DSA to accelerate our LO equations, in conjunction with a iterative Krylov solution method. There are other desirable properties of our algo-

rithm that remain to be tested, e.g., preservation of the maximum principle. In summary, we propose performing the following work to complete this dissertation research:

1. The source iteration method with DSA for the LO solver will be applied to various test problems to ensure a significant reduction in total scattering iterations and the numerically estimated spectral radius in diffusive problems. Problems that provide a mix of optically thick and thin regions, particularly those that require the fix-ups defined in Sec. 4.1 where acceleration may degrade, will be investigated. The acceleration method will be recast as a DSA-preconditioned Krylov method if required for robustness and effectivness.

2. Problems where IMC violates the maximum principle will be simulated with our method. We will demonstrate that our implicit equations preserve the maximum principle, and that our method can produce higher accuracy due to implicit cross section treatment. Such problems will likely require implementation of damping in the Newton iterations.

3. We will numerically demonstrate the ability of our method to preserve the equilibrium diffusion limit. The HOLO method will also be tested with a step discretization in the LO equations to demonstrate inaccuracy in the EDL.

4. The negativity fix-ups discussed in Sec. 4.1 will be investigated for robustness and accuracy. An analytic neutronics problem or a refined deterministic TRT solution will be used to test for accuracy. The ability of the modified ECMC algorithm to reduce noise in the fixup regions will be investigated by measuring sample statistics.

5. The doubly-discontinuous trial space with a consistent spatial closure in the LO equations remains to be implemented. This approach will be compared to the standard LD closure for accuracy, particularly in the case of negative cells.

6. We will investigate the sensitivity of ECMC and the LO equations to parameters, e.g., initial mesh-sizes, adaptive refinement, time step size, history counts, and batch sizes. Additional test problems will be simulated as necessary.

References

[1] J.K. Shultis and W.L. Dunn. *Exploring Monte Carlo Methods*. Academic Press, Burlington, MA 01803, 2012.

[2] J. A. Fleck, Jr. and J. D. Cummings, Jr. An implicit monte carlo scheme for calculating time and frequency dependent nonlinear radiation transport. *J. Comput. Phys.*, 8(3):313–342, December 1971.

[3] NA Gentile. Implicit monte carlo diffusion: An acceleration method for monte carlo time-dependent radiative transfer simulations. *Journal of Computational Physics*, 172(2):543–571, 2001.

[4] Jeffery D Densmore, Kelly G Thompson, and Todd J Urbatsch. A hybrid transport-diffusion monte carlo method for frequency-dependent radiative-transfer simulations. *Journal of Computational Physics*, 231(20):6924–6934, 2012.

[5] Allan B Wollaber, Edward W Larsen, and Jeffery D Densmore. A discrete maximum principle for the implicit monte carlo equations. *Nuclear Science and Engineering*, 173(3):259–275, 2013.

[6] N. A. Gentile and Ben C. Yee. Iterative implicit monte carlo. *Journal of Computational and Theoretical Transport*, 0(0):1–31, 0.

[7] Michael Scott McKinley, Eugene D Brooks III, and Abraham Szoke. Comparison of implicit and symbolic implicit monte carlo line transport with frequency weight vector extension. *Journal of Computational Physics*, 189(1):330–349, 2003.

[8] Jeffery D. Densmore. Asymptotic analysis of the spatial discretization of radiation absorption and re-emission in implicit monte carlo. *Journal of Computational Physics*, 230(4):1116 – 1133, 2011.

[9] J.E. Morel, T.A. Wareing, and K. Smith. Linear-Discontinuous Spatial Differencing Scheme for S_n Radiative Transfer Calculations. *Journal of Computational Physics*, 128:445–462, 1996.

[10] J. Willert, C.T. Kelly, D.A. Knoll, and H. Park. A Hybrid Approach to the Neutron Transport k-Eigenvalue Problem using NDA-based Algorithms. M&C. Sun Valley, ID, 2013.

[11] H. Park, J.D. Densmore, A.B. Wollaber, D.A. Knoll, and R.M. Ramenzahn. Monte Carlo Solution Methods in a Moment-Based Scale-Bridging Algorithm For Thermal Radiative Transfer Problems. M&C. Sun Valley, ID, 2013.

[12] Jeffrey Willert and H. Park. Residual monte carlo high-order solver for moment-based accelerated thermal radiative transfer equations. *Journal of Computational Physics*, 276:405 – 421, 2014.

[13] S.R. Bolding and J.E. Morel. A High-Order Low-Order Algorithm with Exponentially-Convergent Monte Carlo for k-Eigenvalue problems. ANS Winter Meeting. Anaheim, CA, 2014.

[14] Eugene D. Brooks III, Michael Scott McKinley, Frank Daffin, and Abraham Szke. Symbolic implicit monte carlo radiation transport in the difference formulation: a

piecewise constant discretization. *Journal of Computational Physics*, 205(2):737 – 754, 2005.

[15] Eugene D. Brooks III, Abraham Szke, and Jayson D.L. Peterson. "piecewise linear discretization of symbolic implicit monte carlo radiation transport in the difference formulation ". *"Journal of Computational Physics "*, "220"(1):471 – 497, 2006.

[16] E.R. Wolters. *Hybrid Monte Carlo - Deterministic Neutron Transport Methods Using Nonlinear Functionals*. PhD thesis, Michigan, 2011.

[17] J.R. Peterson. Exponentially Convergent Monte Carlo for the 1-d Transport Equation. Master's thesis, Texas A&M, 2014.

[18] T.A. Wareing, E.W. Larsen, and M.L. Adams. Asymptotic Diffusion Accelerated Discontinuous Finite Element Schemes for the S_N Equations in Slab and X-Y Geometries. In *International Topical Meeting on Advances in Mathematics, Computations, Reactor Physics*, volume 3, Pittsburgh, PA, 1991.

[19] T.A. Wareing. *Asymptotic diffusion accelerated discontinuous finite element methods for transport problems*. PhD thesis, Michigan, 1991.

[20] Elmer Eugene Lewis and Warren F Miller. *Computational methods of neutron transport*. John Wiley and Sons, Inc., New York, NY, 1984.

[21] Edward W. Larsen and Jim E. Morel. Advances in discrete-ordinates methodology. *Nuclear Computational Science. Springer Netherlands*, pages 1–84, 2010.